Exp. Theo. NANOTECHNOLOGY 9 (2025) 227-236 https://doi.org/10.56053/9.S.227

Antibacterial efficacy of selenium and zinc selenide nanostructured materials produced through laser ablation technique

Nihal H. Jabr[1,*], *Ahmed K.Abbas*[1], *Isam M.Ibrahim*[2]

[1]Department of Physics, College of Science, University of Wasit, Wasit, Iraq
[2]Department of Physics, College of Science, University of Baghdad, Baghdad, Iraq
[*]) Email: nihal.hussein@uowasit.edu.iq

Received 21/1/2025, *Received in revised form* 2/2/2025, *Accepted* 10/2/2025, *Published* 15/3/2025

This study used pulsed laser ablation at 1064nm with a pulse duration of 9ns and an energy of 50mJ to create selenium and zinc selenide nanostructures. The selenium, zinc, and result selenide sheets are immersed in 3mL of deionized water (D.W.). The XRD patterns confirmed that both ZnSe and Se nanostructures are in a cubic structure. The surface morphology is visualized by FE-SEM. The optical behavior of synthesized Se and ZnSe NPs is investigated using a UV-vis spectrophotometer. This study evaluated the antibacterial activity of these NPs against Staphylococcus aureus and Escherichia coli in vitro. Results indicated that the 3mL dose of Se and ZnSe gave E. coli and S. aureus inhibitions by about 28mm and 12mm for Se and by 15mm and 13mm for ZnSe, respectively. In the wake of the growing antibiotic-resistance in most bacteria, the need for new and novel antibacterial agents becomes imperative for positive public health. Along with the decreasing efficacy of conventional antibiotics, alternative treatments against bacterial infections become needed more than ever. This work involves the synthesis of selenium and zinc selenide nanostructured materials produced via pulsed laser ablation and their related exploration for antibacterial potential to provide the new classes of effective antibacterial agents.

Keywords: ZnSe; Nanoparticles; Laser ablation; Antibacterial.

1. INTRODUCTION

Interest in nanomaterials arises from the extraordinary properties and practical applications in fields such as photodetectors [1], solar cells [2], biological fields [3], catalysis [4], and much more. Among the

nanostructured materials, Se and ZnSe seem to be very promising and have applicability in a wide range of science and technology fields. They are non-toxic, have high binding energy, and large bandgap energy, which allows them to be used in devices like ultraviolet light detectors, solar cells, varistors, and even antibacterial agents. Among the metal oxide nanomaterials, Se and ZnSe nanostructures have exhibited competitive potential against other antibacterial agents due to their biocompatibility, stability, and efficacy even at a lower concentration. Other methods for the synthesis of zinc selenide include chemical vapor deposition [5-14], sol-gel techniques [15], chemical routes [16], and spray pyrolysis [17]; some have used hydrothermal processes [18] and co-precipitation techniques [19]. Among them, pulsed laser ablation of bulk Se and ZnSe in a liquid environment is developed as a simple method for nanostructure synthesis with several advantages like high purity, simplicity, and superior quality of products [20]. Furthermore, PLAL provides the opportunity to prepare tailored nanomaterials with different shapes by varying laser parameters (wavelength, energy, pulse length, and number of laser pulses) and properties of the liquid medium.

In the present study, Se and ZnSe nanoparticles will be prepared by the ablation of a zinc plate in water using Nd:YAG laser and evaluate their antibacterial activity against two types of bacteria. A few research works have been confined to the advantages and mechanisms of nanoparticle synthesis via laser ablation [21-28]. Besner and Richter (2007) worked on the synthesis of colloidal nanoparticles by laser ablation. They showed that variation in the parameter's laser wavelength, pulse duration, and energy can control the size and distribution of the particles. Their findings further pointed out the need for a fine adjustment in these parameters for obtaining the desired characteristics of the nanoparticles [29]. Compagnini et al. have examined the formation of metal nanoparticles by laser ablation in liquids, giving emphasis on the surroundings' role in the properties of such nanoparticles. Thus, their work finally reported that the choice of the liquid medium itself could be very deterministic for nanoparticle size, morphology, and stability, therefore providing insight into the optimum condition of synthesis for a specific application [30]. In 2009, Amendola and Meneghetti demonstrated the use of laser ablation of solids in liquids for the generation of ultrapure nanomaterials. Their paper described the mechanisms underlying the generation of nanoparticles and focused on the advantages derived from the synthesis by laser ablation with respect to other methods: high purity and environmental friendliness [31].

2. EXPERIMENTAL WORK

2.1. Preparation of Se and ZnSe nanoparticles

This work reports the ablation of a Zn target of 99.9% purity by a Q-switching Nd-YAG laser system. The operating parameters of the laser system are as follows: wavelength, 1064 nm; pulse duration, 9 ns; and repetition rate, 6 Hz. This setup avoids the use of a simple stirrer by submerging in three milliliters of water with a small glass container spinning continuously to keep the target from settling. This process is used to avoid the target settling. They used a laser intensity of about 50millijoules but they increased the number of the pulse of lasers during this phase of ablation to 200.

2.2. Portrayal of Se and ZnSe nanoparticles

An X-ray diffraction pattern, XRD, is done for the nanoparticles. This is performed with an X-ray source by Cu-Ke radiation, where 2 is at the angle 20°–80° with a scanning speed of about 5.0000 degrees per minute. We used a Japan-made Philips PW-based apparatus in this study. Moreover, we confirmed the morphology 10keV scanning electron microscopy, MERA3 TES is conducted.

2.3. Antimicrobial potential of Se and ZnSe nanoparticles

They evaluated the efficacy of Se and ZnSe nanoparticles against different strains of Gram-positive and Gram-negative bacteria using an agar diffusion technique according to the methodology. The

combination is incubated for 24 hours in the appropriate atmosphere after using wells with a 6mm diameter and adjusted the doses of nanoparticles. They assessed the treatment's efficacy by measuring the agar diffusion test's resultant inhibitory zone width.

3. RESULTS AND DISCUSSION

Figures 1-3 show the XRD pattern for Se nanoparticles and ZnSe nanoparticles. The diffraction pattern obtained for the sample is matched with the wurtzite crystal structure in the form of a hexagon. There are five different peaks that can be viewed at 2θ values of about 23°, 29°, 41°, 43°and 45. These peaks correspond to the crystallographic planes (100), (101), (110), (102), and (111) for Se, respectively. This indicates that the selenium nanoparticles possess a hexagonal (wurtzite) crystal structure. The XRD pattern closely matches the standard card 65-1876. There are five distinct peaks that may be seen at 2θ values of about 27°, 45°, 53°, 65°, and 72°. These peaks correspond to the crystallographic planes (111), (200), (311), (400), and (331) for ZnSe, respectively. This suggests that the zinc selenide nanoparticles have a cubic (zinc blende) crystal structure. The XRD pattern closely matches the standard card 37-1463. The data presented in the passage refers to specific references [32, 33] where similar XRD patterns and crystallographic analyses can be found, providing additional support and validation for the crystal structures observed in the Se and ZnSe nanoparticles.

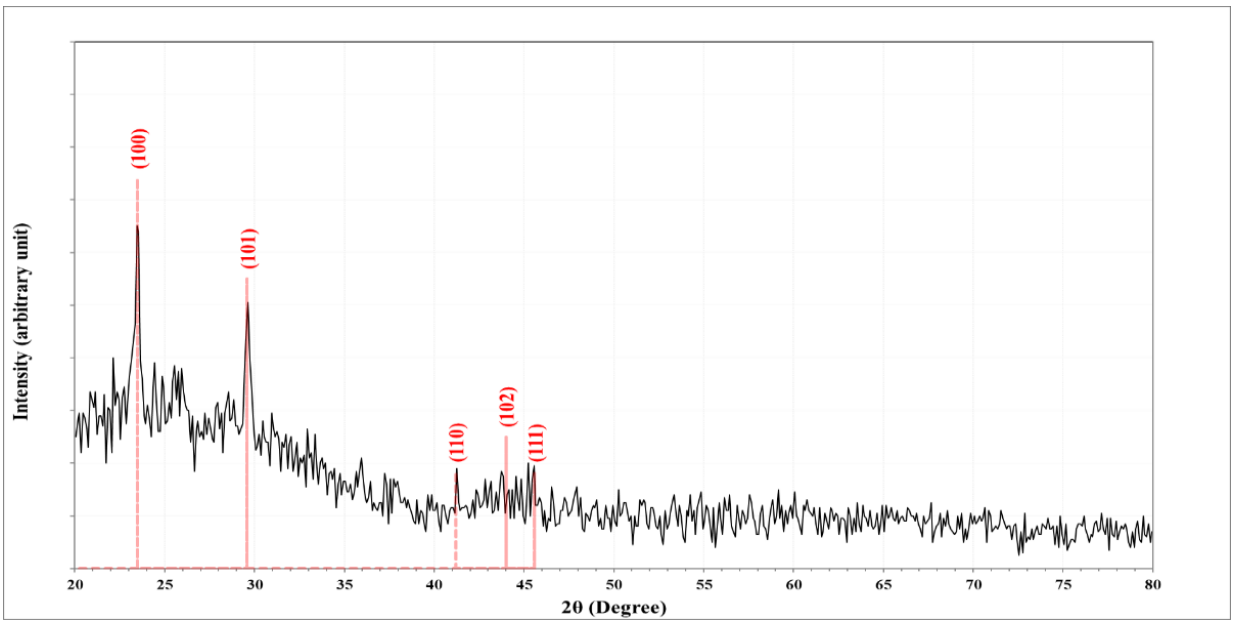

Figure 1 XRD of production of Se nanocrystals using different lasers.

Table 1 Structural parameters of Se.

2θ (Deg.)	FWHM (Deg.)	d_{hkl} (Å)	C.S (nm)	Phase	hkl	Card No
23.486	0.293	3.7849	27.7	Se	(100)	65-1876
29.659	0.399	3.0097	20.6	Se	(101)	65-1876
41.259	0.186	2.1863	45.6	Se	(110)	65-1876
43.761	0.479	2.0670	17.9	Se	(102)	65-1876
45.570	0.373	1.9890	23.1	Se	(111)	65-1876

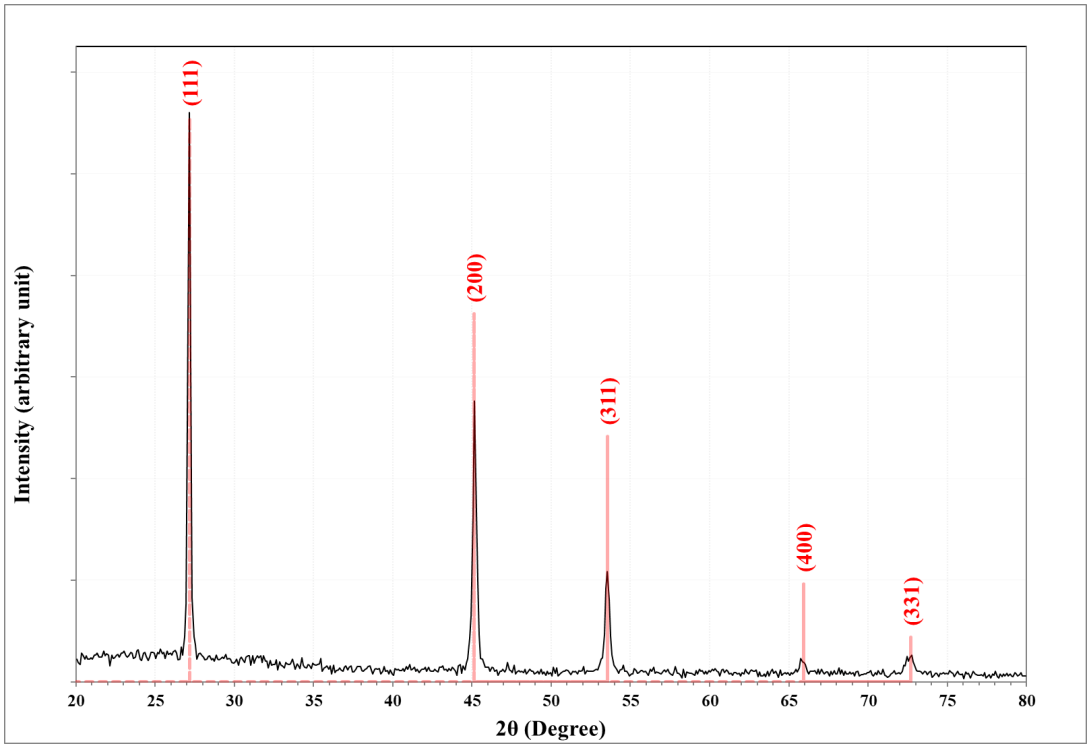

Figure 2 XRD of production of ZnSe nanocrystals using different lasers.

Table 2 Structural parameters of ZnSe.

2θ (Deg.)	FWHM (Deg.)	d_{hkl} (Å)	C.S (nm)	Phase	Hkl	Card No
27.174	0.245	3.2789	33.4	ZnSe	(111)	37-1463
45.154	0.334	2.0064	25.7	ZnSe	(200)	37-1463
53.554	0.334	1.7098	26.	ZnSe	(311)	37-1463
65.785	0.468	1.4184	20.2	ZnSe	(400)	37-1463
72.625	0.646	1.3008	15.3	ZnSe	(331)	37-1463

Figure 3 displays the images of the scanning electron microscope view of selenium nanospheres synthesized through pulsed laser ablation at a wave length of 1064nm and an energy of 50, 100, 150, and 200mJ, using laser pulse 200. It is explicit that dissimilar laser pulses changed the structure of the obtained zinc selenide nanospheres. For example, with a 1064 nm laser wavelength, the particles increase in size as the energy level increases. This implies a direct relationship between the laser energy and the resulting particle size, suggesting that higher energy levels cause more material to be ablated from the target and subsequently form larger particles [34-37].

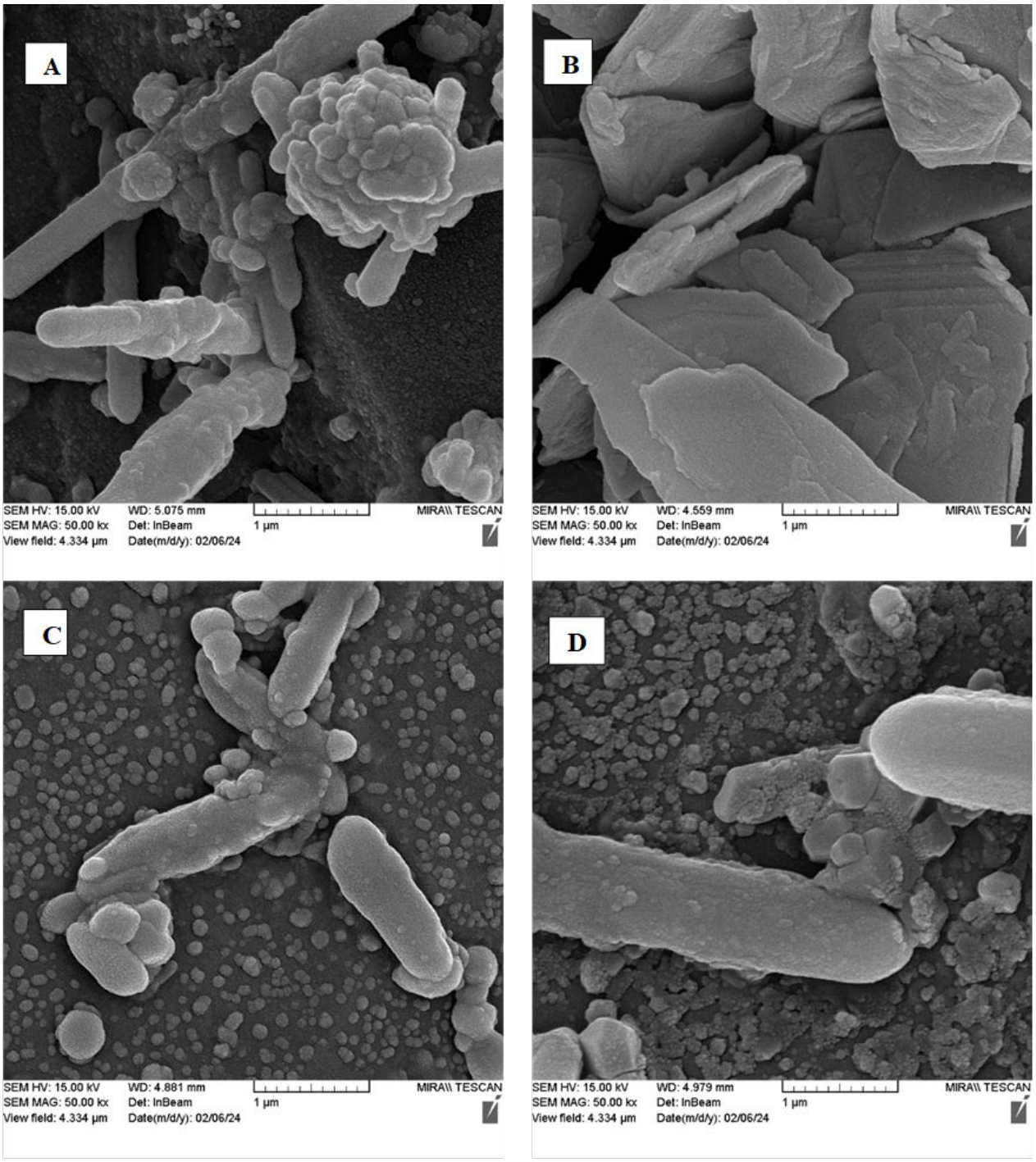

Figure 3 SEM image of Se nanosheets prepared using pulses of different energies: A, energy image at 50 mJ; B, energy image at 100 mJ; C, energy image at 150 mJ; D, energy image at 200 mJ.

Figure 3 displays the images of scanning electron microscope view of zinc selenide nanospheres synthesized by pulsed laser ablation at a wave length of 1064nm and an energy of 50, 100, 150, and 200mJ with the laser pulse of 200. It can be easily explained that the structure of the designed zinc selenide nanospheres is changed with the various laser pulses that are made. The particles increase their size with the increase in the energy level. This relationship between laser energy and particle size can be explained by the fundamental mechanisms of laser ablation, where higher energy levels result in more extensive material removal and subsequent aggregation into larger particles. The work of Zijlstra, Chon, and Gu reinforces the observation that increasing laser energy can lead to larger nanoparticles. Their emphasis on monodispersed also suggests that energy control is crucial for achieving uniform particle sizes, a relevant factor for zinc selenide nanospheres [38].

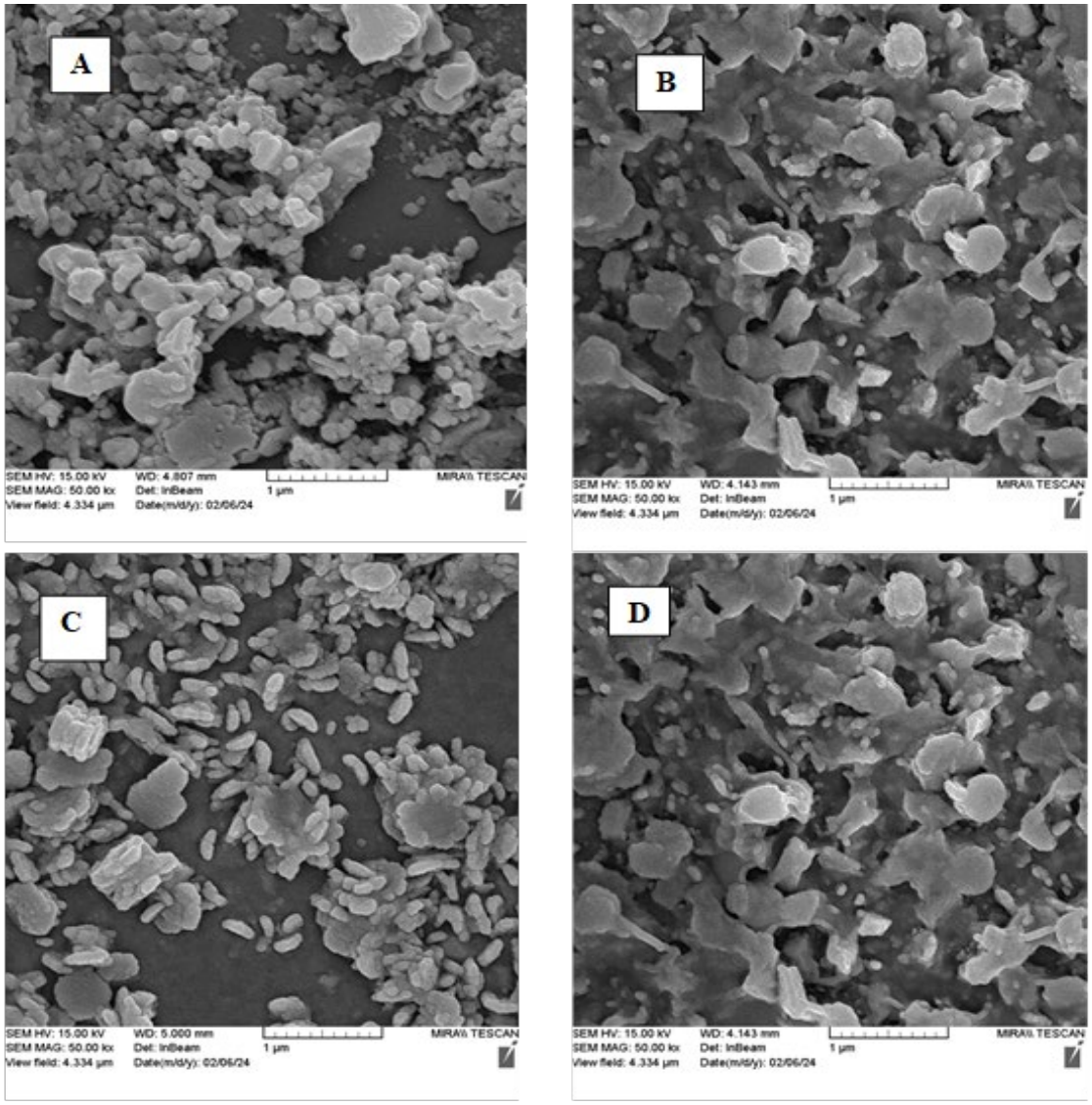

Figure 4 SEM image illustrating ZnSe nanosheets prepared using different pulses. Energy images: (A) 50 mJ, (B) 100 mJ, (C) 150 mJ, and (D) 200 mJ.

The antibacterial activity (see fig. (5)) of Se and ZnSe nanoparticles prepared in distilled water by laser ablation at 50mJ, 200 pulses, and 1064 nm laser wavelength is investigated against both Gram-negative and Gram-positive bacteria. Tables (3) and (4) display the antibacterial properties of ZnSe colloidal nanoparticles against Staph. aureus, Escherichia coli. ZnSe stopped the growth of Staph. aureus bacteria by 12 mm, and E. coli bacteria by 13mm. Inhibition of bacterial growth of Se is about 28mm for Staph. aureus, 15mm for Escherichia. coli. The results showed that gram-positive bacteria (Staphylococcus aureus) are a little bit more sensitive to Se NPs than Escherichia coli. They may have adapted to the different properties of bacterial cell surfaces and their interactions with nanoparticles [39]. Tables (3) and (4) list the inhibition zones obtained. Se and ZnSe nanoparticles demonstrate the preparation's maximum antibacterial activity against Escherichia coli and Staphylococcus. The inhibitory effect of different wavelengths of colloidal Se and ZnSe nanoparticles on Staphylococcus aureus increased as the laser wavelength increased. We can extend this result to the colloidal effects of Se and ZnSe nanoparticles. Damage to the bacteria's membrane wall, however, is further investigated and required. However, the colloidal ZnSe nanoparticles have a fine antibacterial mechanism. The mechanism is still unclear [40-43].

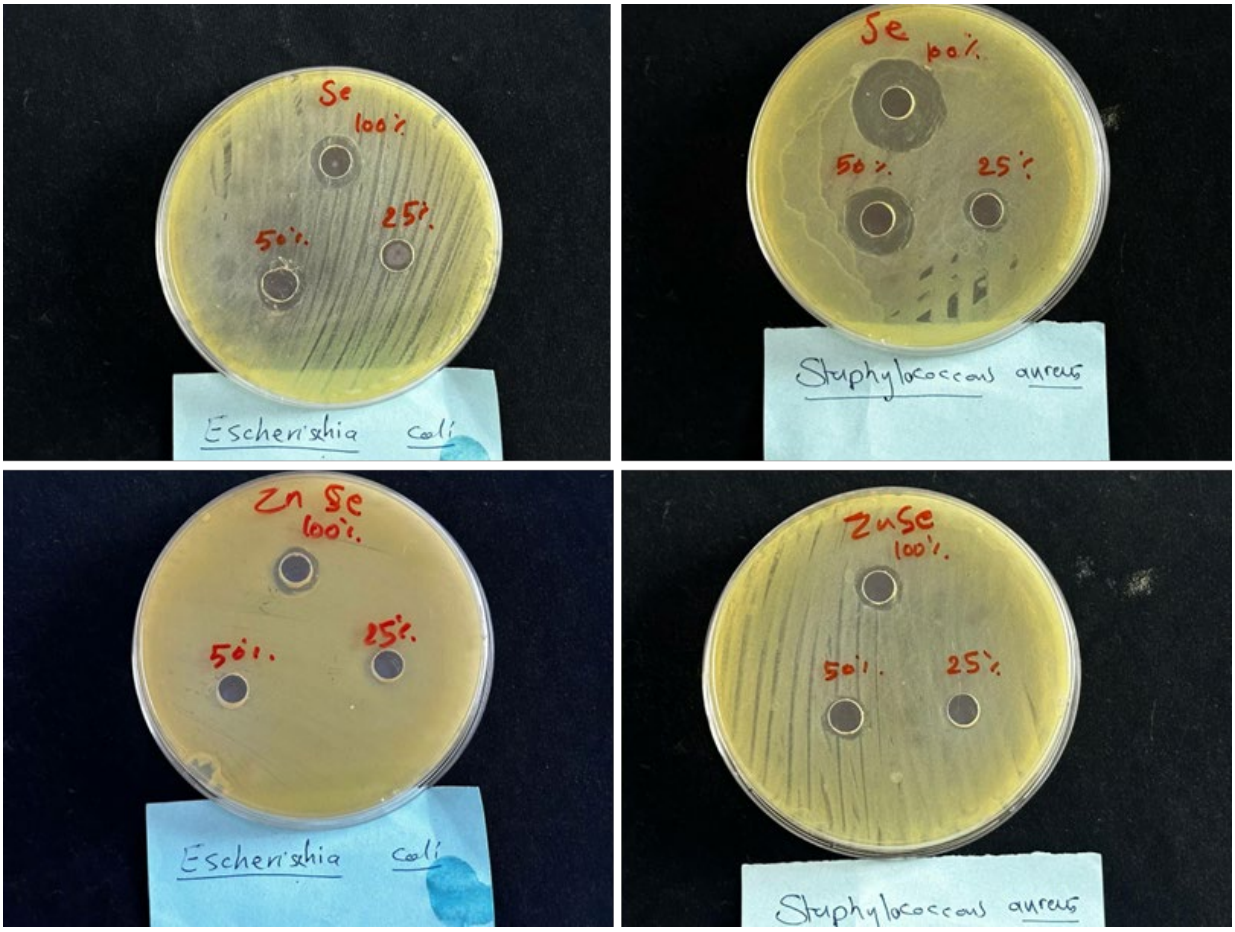

Figure 5 Antibacterial activity of Se and ZnSe nanoparticles prepared in distilled water by laser ablation at 50 mJ,

Table 3 Se nanoparticles reduce E. coli and Staph. aureus.

Se Concentrations	Inhibition zone diameter (mm)	
	E.coli	S.aureus
100%	15	28
50%	14	17
25%	-ue	13

Table 4 ZnSe nanoparticles reduce E. coli and Staph. aureus.

ZnSe Concentrations	Inhibition zone diameter (mm)	
	E.coli	S.aureus
100%	13	12
50%	8	11
25%	-ue	-ue

4. CONCLUSIONS

The utilization of laser pulse ablation in a liquid technique was identified as the optimal and uncomplicated approach for the synthesis of Se and ZnSe nanoparticles. Analysis of the XRD data confirmed the presence of Se and ZnSe nanoparticle peaks. As the laser energy increased, the morphological transformations observed in SEM images indicated a transition from shell-like formations to spherical formations characterized by significant agglomeration. According to tests of antibacterial properties, the effect on Escherichia. Coli was stronger than that on Staph. Aureus. Inhibition zones of 15mm were seen against Escherichia. Coli for Se, and 13 for ZnSe, and a zone of 12mm for ZnSe. An inhibition zone of 28mm was seen for Se against Staphylococcus aureus. Furthermore, these inhibitory effects got stronger as the laser wavelength got longer for both strains of bacteria. This shows that Se and ZnSe nanoparticle materials could be very effective at killing bacteria.

Acknowledgments

The authors express gratitude to their respective universities for providing encouragement and infrastructure.

References

[1] M.A. Green, K. Emery, Y. Hishikawa, W. Warta, E.D. Dunlop, Prog. Photovolt: Res. Appl. 30 (2022) 3
[2] S.L. Shinde, S.T. Gaikwad, S.S. Mali, J. Mater. Sci.: Mater. Electron. 31 (2020) 20377
[3] P. Wick, P. Manser, S. Limbach, R. Dettlaff-Weglikowska, A. Krumeich, P.M. Roth, W. Stark, M. Bruinink, Toxicol. Lett. 168 (2007) 121

[4] X. Wang, S.C. Zhan, D.L. Jiang, Coord. Chem. Rev. 456 (2018) 1
[5] M.R. Jahan, S. Shafique, A.H. Mir, J. Mol. Struct. 1220 (2020) 128027
[6] S.M. Bawazeer, A.A. Al-Hajji, S.M. Yassin, J. Mater. Sci.: Mater. Electron. 30 (2019) 2387
[7] J. Li, W.L. Yang, H. Li, Y.H. Zhang, Y.L. Liu, Mater. Chem. Phys. 128 (2011) 424
[8] H.J. Hassan, A.K. Abbas, I.M. Ibrahim, AIP Conf Proc. 2834 (2023) 090006
[9] A.K.M.A. Islam, M.Z. Rashed, S.S. Islam, J. Nanosci. Nanotechnol. 13 (2013) 4126
[10] S.Y. Huang, Y.L. Liu, W.L. Yang, H. Li, J. Phys. Chem. C 116 (2012) 10589
[11] M.H. Azarshab, N. Fattahi, M.A. Mahdavian, J. Mater. Sci. 56 (2021) 319
[12] K.A. Alkhayal, M.A. Al-Rubeaan, M.S. Al-Saadi, Nanotechnol. Rev. 8 (2019) 241
[13] A.K.M.A. Islam, M.Z. Rashed, S.S. Islam, J. Nanosci. Nanotechnol. 13 (2013) 4385
[14] S.L. Shinde, S.T. Gaikwad, S.S. Mali, Thin Solid Films 666 (2018) 68
[15] P. Wick, P. Manser, S. Limbach, R. Dettlaff-Weglikowska, A. Krumeich, P.M. Roth, W. Stark, M. Bruinink, J. Sol-Gel Sci. Technol. 52 (2009) 284
[16] M.R. Jahan, S. Shafique, A.H. Mir, Chem. Eng. J. 185-186 (2012) 324
[17] A.K. Gupta, A.A. Al-Hajji, S.M. Yassin, J. Mater. Sci.: Mater. Electron. 28 (2017) 7536
[18] S.M. Bawazeer, A.A. Al-Hajji, S.M. Yassin, J. Mater. Sci.: Mater. Electron. 29 (2018) 10254
[19] J. Li, W.L. Yang, H. Li, Y.H. Zhang, Y.L. Liu, J. Nanopart. Res. 15 (2013) 1387
[20] X. Wang, S.C. Zhan, D.L. Jiang, Appl. Surf. Sci. 421 (2017) 591
[21] X. Wang, S.C. Zhan, D.L. Jiang, Prog. Mater. Sci. 88 (2017) 148
[22] A.K. Abbas, I.M. Ibrahim, H. Mayah, H.J. Hassan, J. Phys. Conf. Ser. 2114 (2022) 1
[23] A. Podhorodecki, M.A. Djoumi-Toumi, A.M. Wojciechowski, M. Szymonski, Appl. Phys. A 118 (2015) 1031
[24] K.S. Song, S.M. Yoon, K.K. Lee, J. Korean Phys. Soc. 65 (2014) 744
[25] J. Zhang, Y. Yang, Y. Sun, Nanoscale Res. Lett. 14 (2019) 161
[26] S.Y. Huang, Y.L. Liu, W.L. Yang, H. Li, J. Mater. Sci. 47 (2012) 5631
[27] M.R. Jahan, S. Shafique, A.H. Mir, J. Nanopart. Res. 16 (2014) 2398
[28] A.K. Gupta, A.A. Al-Hajji, S.M. Yassin, Nanotechnol. Rev. 7 (2018) 343
[29] S. Besner, D.B.G. Richter, J. Phys. Chem. C 111 (2007) 7614
[30] G. Compagnini, O. Puglisi, S. Scalese, J. Appl. Phys. 95 (2004) 2006
[31] V. Amendola, M. Meneghetti, Phys. Chem. Chem. Phys. 11 (2009) 3805
[32] M.H. Taku, O. Tatsuki, A.G. Rozhin, S.Y. Shigeru, I. Tsuyohito, S.A. Kulinich, Phys. Chem. Chem. Phys. 18 (2016) 23628
[33] E.Y. Salih, M.F.M. Sabri, S.T. Tan, K. Sulaiman, M.Z. Hussein, S.M. Said, C.C. Yap, J. Nanopart. Res. 21 (2019) 55
[34] A.M. Baranov, D.K. Bogy, Appl. Phys. A 69 (1999) 367
[35] R. Kelly, J. Appl. Phys. 78 (1995) 2758
[36] H.H. Choi, J.H. Sung, S.H. Lee, Thin Solid Films 392 (2001) 151
[37] S.A. Bello, C.O. Kolawole, Nanoscale Res. Lett. 6 (2011) 446
[38] P. Zijlstra, J.W.M. Chon, M. Gu, J. Nanomater. (2008) 204830
[39] I.A. Abdul-Hassan, A.K. Abbas, I.M. Ibrahim, Wuhan Univ. J. Nat. Sci. (2018) 14286
[40] M. Jayadndran, M.M. Haneefa, V. Balasubrammanian, J. Appl. Pharm. Sci. (2015) 105
[41] A. M. Ahmed Alwaise, Raqeeb H. Rajab, Adel A. Mahmood, Mohammed A. Alreshedi, Exp. Theo. NANOTECHNOLOGY 8 (2024) 67
[42] Maria S. da Dunla, Exp. Theo. NANOTECHNOLOGY 8 (2024) 23
[43] Ziyad Khalf Salih, Angham Ayad Kamall-Eldeen, Exp. Theo. NANOTECHNOLOGY 8 (2024) 27